Dimer and polymer metamaterials with alternating electric and magnetic coupling

A. Radkovskaya
Magnetism Division, Faculty of Physics, M. V. Lomonosov Moscow State University, Leninskie Gory, Moscow 119992, Russia

O. Sydoruk
Optical and Semiconductor Devices Group, Electrical and Electronic Engineering (EEE) Department, Imperial College, Exhibition Road, London SW7 2BT, United Kingdom

E. Tatartschuk
Erlangen Graduate School in Advanced Optical Technologies, University of Erlangen-Nuremberg, Paul-Gordan Strasse 6, D-91052 Erlangen, Germany

N. Gneiding
Erlangen Graduate School in Advanced Optical Technologies, University of Erlangen-Nuremberg, Paul-Gordan Strasse 6, D-91052 Erlangen, Germany

C. J. Stevens
Department of Engineering Science, University of Oxford, Parks Road, Oxford OX1 3PJ, United Kingdom

D. J. Edwards
Department of Engineering Science, University of Oxford, Parks Road, Oxford OX1 3PJ, United Kingdom

E. Shamonina*
Optical and Semiconductor Devices Group, Electrical and Electronic Engineering (EEE) Department, Imperial College, Exhibition Road, London SW7 2BT, United Kingdom

(Received 6 April 2011; revised manuscript received 15 July 2011; published 12 September 2011)

Diatomic metamaterials, whose properties can be easily tailored, are studied with the aid of split ring resonator elements. Two different types are shown to exist depending on the coupling within a unit cell being larger or smaller than that between the unit cells. The freedom to adjust the coupling coefficients is used to construct a chain in which coupling alternates between electric and magnetic, between positive and negative. The resulting dispersion characteristics are shown to be radically different from the classical acoustic and optical branches: the upper branch is a forward wave and the lower branch is a backward wave, and even the gap between the two pass bands may disappear yielding infinite phase, finite group-velocity wave. The theory is confirmed both by simulations and experiments.

DOI: 10.1103/PhysRevB.84.125121 PACS number(s): 41.20.Jb, 42.25.Bs, 42.70.Qs, 73.20.Mf

I. INTRODUCTION

Ever since their advent in the early 2000s, metamaterials have attracted attention due to their ability to demonstrate effects not possible in natural materials, prominent examples being negative refraction, superlensing, and cloaking (for recent surveys of the field see, e.g., Refs. 1 and 2). Like natural materials, metamaterials consist of periodically arranged "meta-atoms"—resonant inclusions with tailored magnetic and electric responses. A further analogy between natural and metamaterials is the ability of both to propagate waves due to coupling between individual atoms. Phonons are a prominent example of such waves existing in natural materials. Their metamaterial counterpart is magnetoinductive waves, first studied by Shamonina *et al.*,[3] which propagate due to magnetic coupling between meta-atoms. They were proved to exist on arrays of magnetic meta-atoms such as capacitively loaded loops,[4,5] Swiss rolls,[6] and split ring resonators.[7] They were experimentally observed at radio,[6,8] microwave,[9] and optical frequencies,[10] and used for subwavelength imaging,[11,12] negative refraction,[13] and excitation of surface waves.[14] Their practical applications include signal guiding[5,8,15] and processing,[9,16] as well as detection[17] and amplification[18] for magnetic-resonance imaging.

Electroinductive waves[19,20] propagate on chains of electrically coupled elements in complementary metamaterials, where metal is replaced by dielectric and vice versa. Later studies introduced new terms: instead of magnetoinductive waves they called them magnetization waves[10,21] and magnetic plasmons.[22–24] Further, earlier examples of waves on chains of coupled elements are dipole arrays,[25] optical resonators,[26] and metal nanoparticles.[27]

Relying on the above analogy between natural and metamaterials, we introduced "diatomic" metamaterials[7,28] comprising two different atoms per unit cell. Diatomic metamaterials support two branches of magnetoinductive waves that are similar to optical and acoustic-phonon branches in diatomic solids;[29] the lower branch of magnetoinductive waves is a forward wave and the upper one is a backward wave. Unlike the phonon branches, however, the magnetoinductive backward-wave branch can be either optical or acoustic depending on

the sign of the magnetic coupling coefficient. The existence of two branches in the dispersion was demonstrated to greatly enhance the flexibility in metamaterial design[30] and was successfully employed in parametric amplification.[18,31]

The freedom of tailoring the properties of diatomic metamaterials can be further increased by employing electric in addition to magnetic coupling between the elements. In metamaterials comprising split ring resonators, the type of coupling depends crucially on the mutual orientation of the rings and on the distance between them. A combination of electric and magnetic coupling can yield positive, negative, or zero total coupling coefficients.[32]

In this paper, we propose and study both theoretically and experimentally diatomic metamaterials where the coupling alternates between electric and magnetic from element to element. This is in the spirit mentioned before that metamaterials can do what natural materials cannot. The most striking example is the disappearance of the stop band between the branches. Section II derives the analytical dispersion relation for the waves on diatomic metamaterials. Section III reports on the experiments in the GHz, whereas Sec. IV is concerned with simulations in the THz range. Conclusions are drawn in Sec. V.

II. THEORY OF DIATOMIC METAMATERIALS

This section presents a derivation of the dispersion relation and then considers its properties for two metamaterial realizations: a dimer ("unbalanced") line, where the electric and magnetic coupling coefficients are different, and a polymer ("balanced") line, where the coupling coefficients have equal absolute values.

The elements employed in this study are the familiar split ring resonators (SRRs) having a single gap but now the emphasis is on their relative orientations. We shall consider the "near" configuration where the gaps in neighboring elements (placed at the distance d_{near}) are next to each other, and the "far" configuration (elements at the distance d_{far}) where the gaps are on opposite sides as may be seen in Figs. 1(a) and 1(b). It is fairly obvious that the dominant coupling is electrical in the near case due to the strong coupling between the charges in the vicinity of the gap.[32] In the far case, the gaps being on opposite sides, the dominant coupling is clearly magnetic. When the dimers are formed into a diatomic chain with the period $a = d_{\text{near}} + d_{\text{far}}$ [Fig. 1(c)] the interesting feature is that the coupling alternates between electric and magnetic.

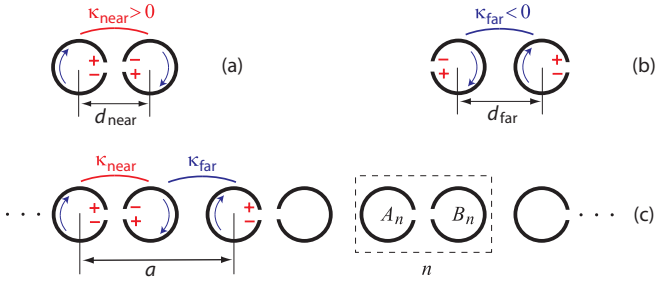

FIG. 1. (Color online) Dimers in the (a) near and (b) far configuration and diatomic chains with alternating type of coupling (c).

Assuming nearest-neighbor interaction, the Lagrangian[33] corresponding to the infinite diatomic chain of Fig. 1(c) may be written as follows:

$$\mathcal{L} = \sum_n \left[\frac{L}{2}\left(\dot{p}_n^2 + \dot{q}_n^2\right) - \frac{p_n^2 + q_n^2}{2C} + M\dot{p}_n\dot{q}_{n-1} - \frac{p_n q_n}{K} \right], \tag{1}$$

where p_n and q_n are the charges on the elements constituting the nth unit cell, L and C are the self-inductance and capacitance, M is the mutual inductance, K characterizes the mutual capacitance, and the dot denotes the time derivative. Using the Euler equations for dissipative systems, with R being the ohmic resistance,

$$\frac{d}{dt}\left(\frac{\partial \mathcal{L}}{\partial \dot{\alpha}_n}\right) - \frac{\partial \mathcal{L}}{\partial \alpha_n} = -R\dot{\alpha}_n, \qquad \alpha = p,q, \tag{2}$$

we arrive at Kirchhoff's equations for currents $A_n = \dot{p}_n$ and $B_n = \dot{q}_n$,

$$\begin{aligned} Z_0 A_n - i\omega M B_{n-1} - \frac{1}{i\omega K} B_n = 0, \\ Z_0 B_n - \frac{1}{i\omega K} A_n - i\omega M A_{n+1} = 0, \end{aligned} \tag{3}$$

where $Z_0 = R - i(\omega L - 1/\omega C)$ denotes the self-impedance and ω is the frequency.

Assuming propagating solutions for both sublattices, $A_n = A\exp[i(kan - \omega t)]$ and $B_n = B\exp[i(kan - \omega t)]$ with complex amplitudes, A and B, and a complex wave number $k = k' + ik''$, we finally obtain the dispersion equation in the form

$$4\zeta^2 = \kappa_{\text{far}}^2 + \kappa_{\text{near}}^2 \nu^4 + 2\kappa_{\text{far}}\kappa_{\text{near}}\nu^2 \cos ka, \tag{4}$$

and the relationship between the amplitudes of currents within the same unit cell as

$$B/A = -2\zeta[\kappa_{\text{far}}\exp(-ika) + \kappa_{\text{near}}\nu^2]^{-1}, \tag{5}$$

where $\zeta = (1 - \nu^2 + i\nu Q^{-1})$ denotes the self-impedance of the SRR normalized to ωL, $\nu = \omega_0/\omega$ is the reciprocal frequency normalized to the resonant frequency $\omega_0 = 1/\sqrt{LC}$, $\kappa_{\text{far}} = 2M/L$ ($\kappa_{\text{near}} = -2C/K$) is the magnetic (electric) coupling coefficient, and $Q = \omega_0 L/R$ is the quality factor. Note that for the planar configuration[32] of Fig. 1(c), $\kappa_{\text{far}} < 0$ whereas $\kappa_{\text{near}} > 0$.

We shall now make a distinction between the dimer unbalanced line, with nonequal values of the electric and magnetic coupling, $\kappa_{\text{far}} \neq -\kappa_{\text{near}}$, and the polymer balanced one, where the interelement coupling is constant in magnitude but alternates in sign from element to element.

Note that retardation is disregarded because we are concerned with slow waves and the distance between the elements is small. Retardation should of course be taken into account when the length of the structure is large relative to the free space wavelength as shown by Weber and Ford[34] and, in the metamaterial context, by Zhuromskyy *et al.*[35]

A. Unbalanced dimer line

The dimer, two elements coupled to each other, has two discrete resonant frequencies. If there is a chain made up by

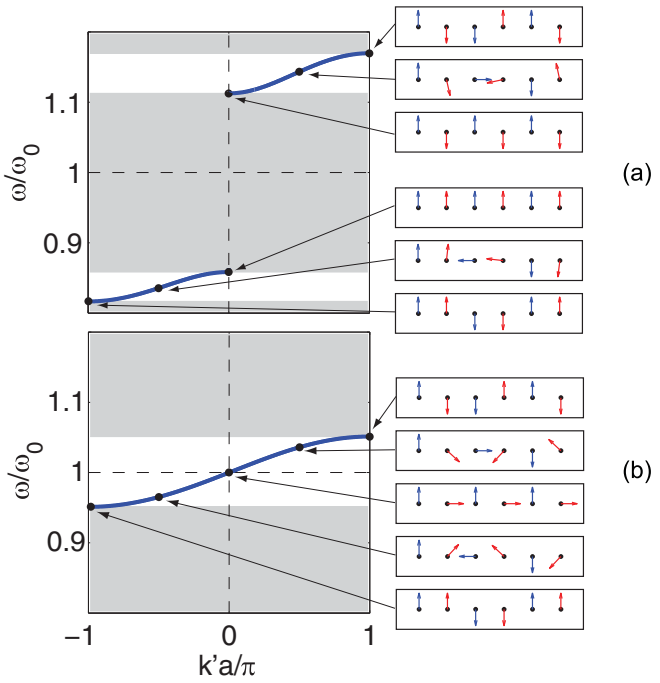

FIG. 2. (Color online) Dispersion diagrams for a diatomic chain showing magnetic-field phasors in the insets for (a) unbalanced and (b) balanced line.

these dimers, each frequency will spread into a band, and very likely, there will be a stop band between the two pass bands. In the absence of loss, the two bands are given as

$$\sqrt{\frac{2 \pm \kappa_{\text{near}}}{2 - \kappa_{\text{far}}}} \leqslant \frac{\omega_{\pm}}{\omega_0} \leqslant \sqrt{\frac{2 \pm \kappa_{\text{near}}}{2 + \kappa_{\text{far}}}}. \tag{6}$$

The corresponding dispersion curves for $\kappa_{\text{near}} = 0.6$, $\kappa_{\text{far}} = -0.1$ are shown in Fig. 2(a). Note that there is no propagation at the resonant frequency ω_0.

In a diatomic chain, one would expect a forward wave in the lower branch and a backward wave in the upper branch. Such expectation is based on the century-old solution for the dispersion equation of vibrating ions in which the lower acoustic branch is a forward wave and the upper optical branch is a backward wave.[29] Similar relationships were found more recently in metamaterial chains based on purely magnetic coupling.[7,28] But now the roles are interchanged, and in Fig. 2(a), the forward wave is in the upper branch and the backward wave is in the lower branch.

It is useful to interpret the unbalanced structure with the dominant electric coupling as a chain of electric dimers, each consisting of two SRRs coupled electrically and having two eigenfrequencies, the lower one (with currents in the two rings being in phase) and the upper one (in antiphase). Around each of the two frequencies there is a pass band of the magnetoinductive wave due to the negative magnetic coupling between the dimers so the lower branch is a backward wave, whereas the upper branch is a forward wave. The insets in Fig. 2(a) show the phasors of the magnetic field at the center of the rings in subsequent elements. They are calculated analytically at a few typical points of the dispersion curve, at $k'a = 0, \pm\pi/2, \pm\pi$. The first phasor is always taken as vertical and the others are relative to the first one. If we look for example at the upper branch we would expect from simple physical arguments that the two elements within the unit cell are always in antiphase. This is true indeed for $k'a = \pi$ and $k'a = 0$ but there is a slight discrepancy at $k'a = \pi/2$. The phase difference is 167° instead of 180°. We can draw similar conclusions from the insets for the lower branch. The magnetic fields within the same dimer are in phase at $k'a = 0$ and $-\pi$ whereas at $k'a = -\pi/2$ they are out of phase by 7°. We have also done the phasor calculations reducing gradually the magnetic coupling. It turns out that the phasors behave in the predicted manner for sufficiently small magnetic coupling.

B. Balanced polymer line

If $\kappa_{\text{far}} = -\kappa_{\text{near}}$, the dispersion curve changes dramatically. The stop band around the resonant frequency closes up as may be seen in Fig. 2(b). An interesting consequence is that at the resonant frequency a mode can propagate with infinite phase velocity but nonzero group velocity. The phasors of the magnetic field along the chain can be seen to differ from those for the unbalanced line. For the balanced case there is a bigger variety of phase differences between the elements in the unit cell. For $k'a = \pi$ it is 180°, for $k'a = \pi/2$ it is 135°, for $k'a = 0$ it is 90°, for $k'a = -\pi/2$ it is 45°, and for $k'a = -\pi$ it is 0°. There is a nice progression from 180° down to 0°. We need to mention here the special case of $k'a = 0$. It is a special case because in the vicinity of $k'a = 0$ the phase undergoes a singularity, a familiar phenomenon in resonant systems. The correct value of $\pi/2$ can be obtained by assuming a small loss that will remove the singularity.

There is no doubt that the unbalanced configuration can be regarded with good conscience as a chain of coupled dimers since the coupling within the dimer is much stronger than that between the dimers. A brief look at the dispersion diagram will show that the properties of the dimer dominate. The dispersion curves are split. However, in the balanced configuration the role of the dimers has greatly diminished. The structure has only a very limited memory of the properties of the dimer. It is of course not a uniform structure, the coupling alternates between electric and magnetic, but there is an overall uniformity corroborated by the existence of a single dispersion curve. In contrast to the dimer line, we may call this a polymer line.

III. EXPERIMENTS WITH DIATOMIC LINES IN THE GIGAHERTZ RANGE

To verify the theoretical predictions, we realized and studied experimentally both dimer and polymer lines. The elements in our experiments were copper SRRs shown in Fig. 3(a). The ring dimensions were $r = 10$ mm, $h = 5$ mm, $w = 1$ mm, $g = 1.5$ mm, the corresponding resonant frequency was $\omega_0/2\pi = (1.78 \pm 0.01)$ GHz, and the quality factor was $Q = 34 \pm 4$. The measurements were done by putting small transmitter and receiver loops close to the elements and measuring the currents at 1601 frequency points between 1 and 3 GHz using a network analyzer (HP 8753ES), a method actively used for studying metamaterial properties.[30]

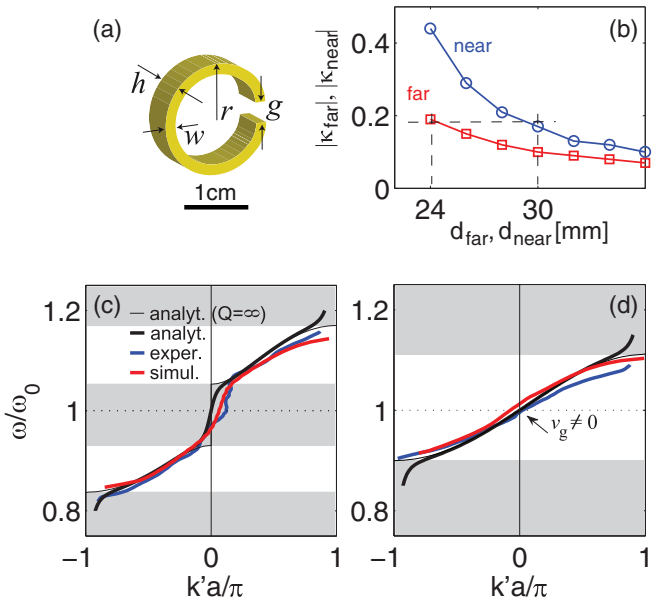

FIG. 3. (Color online) GHz element (a). Dimer coupling versus distance (b). Dispersion diagrams for diatomic chains determined in four different ways for the unbalanced (c) and balanced line (d). Shaded areas show the stop bands in the absence of losses.

The unbalanced GHz structure is an equidistant diatomic chain of 18 SRRs with the unit cell $a = 48$ mm. The coupling coefficients between the elements of the dimer were measured in both configurations shown in Figs. 1(a) and 1(b). One of the elements was excited by a transmitter loop and a receiver measured the currents in both elements. The values of the coupling coefficients (using the technique of Ref. 32) were found as $\kappa_{\text{near}} = 0.45$ and $\kappa_{\text{far}} = -0.21$.

To determine the dispersion characteristics experimentally, it was necessary to measure the relative phase and magnitude of the current in all the elements of the chain. This was done by exciting the first element by a transmitter loop and measuring the magnetic field in each element by translating the receiver coil. The dispersion characteristics were extracted from the measured currents using the expression[7,36]

$$\cos ka = \frac{I_{n+1} + I_{n-1}}{2I_n}. \tag{7}$$

Here I_n is either A_n or B_n, which can be shown to be valid for finite chains exhibiting reflections from the end of the structure.

The dispersion was also determined in a similar manner from numerical data obtained using CST Microwave Studio.[37] In simulations, the first SRR was excited via a port (a voltage source placed in the gap) and the signals (A_n and B_n) were measured by magnetic-field probes placed in the centers of the SRRs.[32] A third way of finding the dispersion curves is to substitute into our dispersion equation (4) the measured values of ω_0, Q, κ_{far}, and κ_{near}. The fourth way is actually the same as the third one but taking $Q = \infty$. This yields the dispersion curve we have already plotted in Fig. 2 for different parameters.

In the balanced line, the value of κ_{near} was reduced to 0.21. This was achieved by increasing the distance for pairs of SRRs with gaps facing each other (near) from 24 to 30 mm [see Fig. 3(b) for the dependence of experimentally measured coupling constants on the distance between the elements and with the dashed lines explaining our choice for d_{near} in the balanced line].

All four resulting dispersion characteristics for the unbalanced and balanced chain are shown in Figs. 3(c) and 3(d). For the unbalanced line, as expected, there are two pass bands surrounded by stop bands. The positions of the stop bands are determined from the lossless analytical model. Because of overlap, the corresponding dispersion curves (thin black lines) can only be seen near the edges of the zone where they have zero slope. The other three curves represent the lossy analytical (black lines), the experimental (blue lines) and the simulated (red lines) results. All four curves may be seen to be very close to each other. Note that in the presence of losses propagation is allowed in the stop bands but those propagating waves are highly attenuated, so the experimental errors are bound to be higher there.

IV. SIMULATIONS OF DIATOMIC LINES IN THE TERAHERTZ RANGE

To verify that our model is also applicable to nanostructured metamaterials at terahertz frequencies, we studied numerically and analytically another set of structures comprising 60 SRRs of rectangular shape shown in Fig. 4(a). SRR dimensions were $l_1 = 400$ nm, $l_2 = 250$ nm, $h = 75$ nm, $w = 50$ nm, and $g = 50$ nm. The resonant frequency was 104 THz, and the quality factor, $Q = 13$. For the unbalanced line ($a = 600$ nm) the extracted values of κ_{near} and κ_{far} were 0.67 and -0.15 at the distance of 300 nm between the SRR centers. For the balanced line, the electric coupling was made equal to the

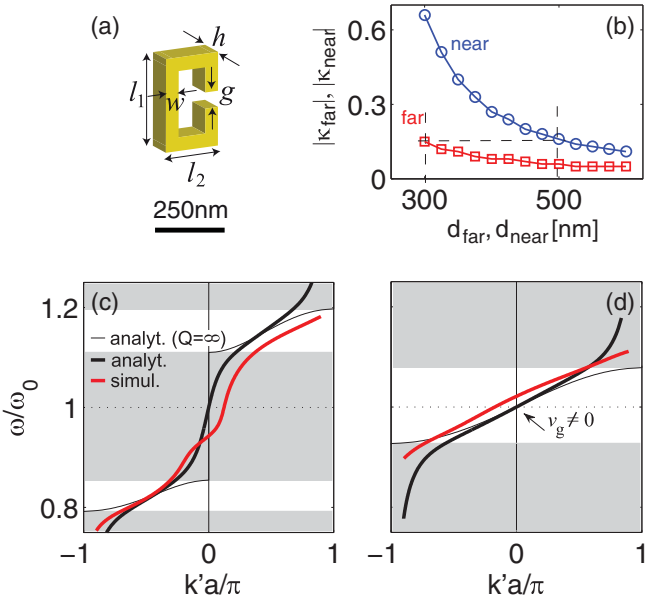

FIG. 4. (Color online) IR element (a). Dimer coupling versus distance (b). Dispersion diagrams for diatomic chains determined in three different ways for the unbalanced (c) and balanced line (d). Shaded areas show the stop bands in the absence of losses.

magnetic coupling by increasing the distance between the centers of electrically coupled SRRs to 500 nm [see Fig. 4(b)]. Figures 4(c) and 4(d) show the dispersion characteristics for the unbalanced and balanced chain demonstrating again good agreement between simulations and analytic calculations. The same qualitative behavior can be seen to occur both in the GHz and in the THz frequency range.

V. CONCLUSIONS

A diatomic metamaterial chain in which the coupling between the elements is adjustable between positive and negative values has been studied. It has been shown that the arising dispersion characteristics differ drastically from the well-known classical relations with a lower acoustic and an upper optical branch. A division into two basic types has been affected depending on the coupling between the elements in a dimer being weaker or stronger than that between dimers. In the special case when neighboring coupling coefficients are equal but opposite in sign, a wave has been found that has infinite phase but finite group velocity, analogously to the microstrip, left-handed transmission line investigated by Caloz and Itoh.[38]

The increased flexibility in designing the coupling coefficient will open a wide range of applications, in particular it offers an alternative realization of an antenna that can be scanned from backfire to endfire.[39] The adjustability of the gap between the pass bands will also aid the design of parametric amplifiers that can be used both in magnetic-resonance imaging[18] and in compensating attenuation in a line.[31,40,41] The theory has been confirmed both by numerical simulation and by experiment at GHz frequencies, and by simulation at THz frequencies.

ACKNOWLEDGMENTS

Financial support of the Russian Foundation for Basic Research, the Royal Society, the Royal Academy of Engineering, the German Research Foundation, and the Leverhulme Trust is gratefully acknowledged.

*e.shamonina@imperial.ac.uk

[1] *Metamaterials: Theory, Design and Applications*, edited by T. J. Cui, D. R. Smith, and R. Liu (Springer, New York, 2009).
[2] L. Solymar and E. Shamonina, *Waves in Metamaterials* (Oxford University Press, Oxford, 2009).
[3] E. Shamonina, V. A. Kalinin, K. H. Ringhofer, and L. Solymar, J. Appl. Phys. **92**, 6252 (2002).
[4] M. C. K. Wiltshire, J. V. Hajnal, J. B. Pendry, D. J. Edwards, and C. J. Stevens, Opt. Express **11**, 709 (2003).
[5] R. R. A. Syms, I. R. Young, and L. Solymar, J. Phys. D **39**, 1945 (2006).
[6] M. C. K. Wiltshire, E. Shamonina, I. R. Young, and L. Solymar, J. Appl. Phys. **95**, 4488 (2004).
[7] A. Radkovskaya, O. Sydoruk, M. Shamonin, C. J. Stevens, G. Faulkner, D. J. Edwards, E. Shamonina, and L. Solymar, IET Microw. Antennas Propag. **1**, 80 (2007).
[8] M. C. K. Wiltshire, E. Shamonina, I. R. Young, and L. Solymar, Electron. Lett. **39**, 215 (2003).
[9] M. J. Freire, R. Marques, F. Medina, M. A. G. Laso, and F. Martin, Appl. Phys. Lett. **85**, 4439 (2004).
[10] G. Dolling, M. Wegener, A. Schädle, S. Burger, and S. Linden, Appl. Phys. Lett. **89**, 231118 (2006).
[11] M. J. Freire and R. Marques, Appl. Phys. Lett. **86**, 182505 (2005).
[12] O. Sydoruk, M. Shamonin, A. Radkovskaya, O. Zhuromskyy, E. Shamonina, R. Trautner, C. J. Stevens, G. Faulkner, D. J. Edwards, and L. Solymar, J. Appl. Phys. **101**, 073903 (2007).
[13] R. R. A. Syms, E. Shamonina, and L. Solymar, Eur. Phys. J. B **46**, 301 (2005).
[14] A. Radkovskaya, E. Tatartschuk, O. Sydoruk, E. Shamonina, C. J. Stevens, D. J. Edwards, and L. Solymar, Phys. Rev. B **82**, 045430 (2010).
[15] R. R. A. Syms, L. Solymar, I. R. Young, and T. Floume, J. Phys. D **43**, 055102 (2010).
[16] R. R. A. Syms, E. Shamonina, and L. Solymar, IEE Proc. Microw. Ant. Prop. **153**, 111 (2006).
[17] L. Solymar, O. Zhuromskyy, O. Sydoruk, E. Shamonina, I. R. Young, and R. R. A. Syms, J. Appl. Phys. **99**, 123908 (2006).
[18] R. R. A. Syms, Metamaterials **2**, 122 (2008).
[19] J. D. Baena, J. Bonache, F. Martin, R. Marques, F. Falcone, T. Lopetegi, M. A. G. Laso, J. Garcia-Garcia, M. F. Portillo, and M. Sorolla, IEEE Trans. MTT **53**, 1451 (2005).
[20] M. Beruete, M. J. Freire, R. Marques, J. D. Baena, and M. Sorolla, in *International Conference on Photonic and Electromagnetic Crystal Structures (PECS-VI)* (Aghia Pelaghia, Crete, Greece, 2005).
[21] M. Decker, S. Burger, S. Linden, and M. Wegener, Phys. Rev. B **80**, 193102 (2009).
[22] H. Liu, D. A. Genov, D. M. Wu, Y. M. Liu, J. M. Steele, C. Sun, S. N. Zhu, and X. Zhang, Phys. Rev. Lett. **97**, 243902 (2006).
[23] H. Liu, D. A. Genov, D. M. Wu, Y. M. Liu, Z. W. Liu, C. Sun, S. N. Zhu, and X. Zhang, Phys. Rev. B **76**, 073101 (2007).
[24] T. Li, R. X. Ye, C. Li, H. Liu, S. M. Wang, J. X. Cao, S. N. Zhu, and X. Zhang, Opt. Express **17**, 11486 (2009).
[25] J. Shefer, IEEE Trans. MTT **11**, 55 (1963).
[26] A. Yariv, Y. Xu, R. K. Lee, and A. Scherer, Opt. Lett. **24**, 711 (1999).
[27] M. Quinten, A. Leitner, J. R. Krenn, and F. R. Aussenegg, Opt. Lett. **23**, 1331 (1998).
[28] O. Sydoruk, O. Zhuromskyy, E. Shamonina, and L. Solymar, Appl. Phys. Lett. **87**, 072501 (2005).
[29] C. Kittel, *Introduction to Solid State Physics* (John Wiley, New York, 1953).
[30] O. Sydoruk, A. Radkovskaya, O. Zhuromskyy, E. Shamonina, M. Shamonin, C. J. Stevens, G. Faulkner, D. J. Edwards, and L. Solymar, Phys. Rev. B **73**, 224406 (2006).
[31] O. Sydoruk, E. Shamonina, and L. Solymar, J. Phys. D **40** (2007).
[32] F. Hesmer, E. Tatartschuk, O. Zhuromskyy, A. Radkovskaya, M. Shamonin, T. Hao, C. J. Stevens, G. Faulkner, D. J. Edwards, and E. Shamonina, Phys. Status Solidi B **244**, 1170 (2007).

[33]L. D. Landau and E. M. Lifschitz, *Electrodynamics of Continuous Media* (Pergamon, Oxford, 1984).
[34]W. H. Weber and G. W. Ford, Phys. Rev. B **70**, 125429 (2004).
[35]O. Zhuromskyy, O. Sydoruk, E. Shamonina, and L. Solymar, J. Appl. Phys. **106**, 104908 (2009).
[36]A. Andryieuski, R. Malureanu, and A. V. Lavrinenko, Phys. Rev. B **80**, 193101 (2009).
[37][http://www.cst.com].
[38]C. Caloz and T. Itoh, *Electromagnetic Metamaterials: Transmission Line Theory and Microwave Applications* (Wiley Interscience, New York, 2006).
[39]N. Yang, C. Caloz, and K. Wu, IEEE Trans. Microwave Theory Tech. **58**, 2619 (2010).
[40]A. K. Popov and V. M. Shalaev, Opt. Lett. **31**, 2169 (2006).
[41]O. Sydoruk, V. A. Kalinin, and E. Shamonina, Phys. Status Solidi B **244**, 1176 (2007).